Design of Three-Phase Relative Permeability Experiments

H. Urkedal,[1] K. Langaas,[1] J.E. Nordtvedt,[1] and A.T. Watson[2]

[1] RF – Rogaland Research, P.O. Box 2503 Ullandhaug, N-4004 Stavanger, Norway
[2] Texas A&M University, Dept. of Chem. Eng., College Station, TX 77843-3122, USA

Abstract

This paper presents, for the first time, a systematic approach to the selection of experimental designs leading to accurate determination of the three-phase relative permeability functions. The approach is based on a linearized covariance analysis which is utilized to determine the confidence intervals on estimated relative permeabilities. These confidence intervals define the accuracy with which the relative permeabilities can be determined for the given data, their acccuracy, and the chosen flooding scenario. In this paper, the confidence intervals are utilized to quantitatively assess the utility of different designs towards accurate three-phase relative permeability determination. For the cases considered here, we demonstrate that accurate estimates may be obtained in the parts of the saturation region which are reflected in the experimental data.

Introduction

Two- and three-phase relative permeabilities are important properties of porous media. In order to perform reservoir forcasting in a multi-phase situation, these functions will have to be specified at all locations within the considered porous structure. Since one usually does not have sufficient field data available for analyses leading to relative permeability estimates, the properties are most commonly inferred through analyses of data acquired during some process imposed on a sample extracted from the reservoir. These data will typically be from some type of displacement experiment, in which one or several fluids are injected into a saturated core. The data (called flooding data hereafter) may comprise fluid production and pressure drop as a function of time, and, possibly, *in situ* saturation and/or phase pressures as functions of time and position.

For two-phase situations, a sound approach has been developed for determining the relative permeabilities[15]. In this approach, the relative permeability functions are determined through a solution of a series of linear inequality constrained least-squares problems (a regression-based approach), the idea being that the properties are chosen such that the measured flooding data "match" the ones calculated using a numerical simulator. In each step in the regression-based approach, the functions are represented by a set of parameters. For a number of two-phase experimental scenarios, it has been demonstrated that relative permeability and capillary pressure functions may be accurately determined utilizing this approach, e.g., dynamic displacement experiments[12, 6], centrifuge experiments[7], and modified steady-state experiments[8]. This methodology has proven to be quite superior to the more frequently used JBN method[3] (see analysis in [11]), and has the advantage of being able to determine both capillary pressure and relative permeability functions simultaneously from a given set of data. One particularly important characteristic of the regression-based

approach is that it allows for the determination of *functions*, rather than sets of discrete points, the latter being the output of the JBN-type interpretation of displacement data.

In the three-phase case, however, the estimation of functions, as opposed to sets of discrete points, has just recently been addressed[5]. Most of the effort up to now has been concentrated on extending the JBN-method to three-phase situations (see, e.g.,[13]), and utilization of the steady-state technique (see, e.g.,[9, 10]). Both these methods provides relative permeability values (i.e., *points*) along one or several trajectories in the three-phase diagram. However, the entire relative permeability functions need to be determined if the estimates should be of any utility in reservoir simulation or forecasting. Furthermore, as the capillary pressure is neglected in both these approaches, the relative permeability points determined from these analyses will suffer from this modeling error[4]. Although the regression-based approach circumvents previous problems, the experiments need to be carried out in such a manner that sufficient information is extracted for accurate estimation of the three-phase relative permeability functions over a relatively large saturation region.

This paper addresses the design of three-phase experiments leading to accurate determination of relative permeability functions. We will investigate different types of data and different flooding scenarios and their impact on the accuracy of the estimated relative permebility functions.

Design of Experiments

There is a huge variety of ways of performing experiments leading to three-phase relative permeability estimates. For example, one may inject one, two, or three phases simultaneously into a core sample, or conduct some constant pressure drop experiments. Obviously, it is desirable to keep the number of experiments needed for three-phase relative permeability determination as low as possible, yet the accuracy with which these functions are determined as high as possible. This section presents a systematic approach for designing the three-phase experiments leading to accurate determination of the three-phase relative permeability functions. By *design* of three-phase experiments, we mean the manner in which the experiments are conducted (e.g., a series of injections of gas into a sample initially saturated with oil and water) *and* the experimental flooding data measured (both type of data and location of each datapoint (in time and/or space), as well as the accuracy with which the data are measured).

The evaluation of the designs will be based upon measures of the accuracy with which the relative permeabilities may be determined from a given set of data. In the two-phase situation, accuracy measures have been obtained through a linearized covariance analysis[4]. In the covariance analysis, it is assumed that a mathematical model capable of describing the physics of the considered process exists. It is further assumed that we can adequately represent the relative permeability functions by a set of parameters, that the mathematical model is linear in these parameters near the solution, and, finally, that the errors in the measurements are additive with zero mean and a given standard deviation; see Kerig and Watson[4] for details. The parameters are taken to be estimated through solution of the constrained least-squares problem defined by:

$$min \ J(\vec{\beta}) \ = \ [\vec{Y}_m - \vec{Y}_s(\vec{\beta})]^T \mathbf{W} [\vec{Y}_m - \vec{Y}_s(\vec{\beta})] \tag{1}$$

$$subject \ to \ \mathbf{G}\vec{\beta} \ \geq \ \vec{b}. \tag{2}$$

Here, $\vec{Y}_m$ is the vector of measured data, and $\vec{Y}_s(\vec{\beta})$ is the corresponding vector of simulated quantities. $\mathbf{W}$ is the weighting matrix, and $\vec{\beta}$ contains the parameters in the functional representation of the relative permeability and/or capillary pressure functions. By choosing $\mathbf{W}$ to be the inverse of the covariance matrix of the measurements $(\mathbf{W} = \mathbf{C}^{-1})$, the solution of Eqs. 1- 2 becomes the maximum-likelihood estimates of the parameters, $\vec{\beta}$[1]. It can then be shown that the covariance matrix of the parameter estimates is given by[4]

$$\mathbf{P} = (\mathbf{A}^T \mathbf{C}^{-1} \mathbf{A})^{-1}, \tag{3}$$

where $\mathbf{A}$ is the sensitivity matrix (with elements $a_{ij} = \partial Y_{s,i}/\partial \beta_j$), and $\mathbf{C}$ is the covariance matrix of the measurements. Linearizing the relative permeability functions around the true parameter values, a (pointwise) relative permeability confidence interval can be calculated for any saturation value.

This analysis has been used for determining confidence intervals for the estimates of the relative permeability functions for a number of two-phase situations, see[6, 7, 8, 11]. Also, three-phase situations have recently been considered[5]. In this work, we have extended the analysis to three-phase situations in which data from several three-phase experiments can be considered simultaneously.

Note that these accuracy measures are obtained from knowledge of the simulated experimental data $(\vec{Y}_s(\vec{\beta}))$, the parameters in the functional representation of the relative permeabilities $(\vec{\beta})$, and the covariance matrix of the measurements $(\mathbf{C})$. Thus, to determine the accuracy with which the relative permeabilities may be determined from a particular experimental design, the core sample and fluid properties will first have to be selected, along with injection strategies, types of data and time, position, and accuracies with which these measurements are going to be acquired, and finally, the parameters in the functional representation of the relative permeabilities. Then, using this selected experimental design, $\vec{Y}_s(\vec{\beta})$ can be calculated using a numerical simulator; in this work, $\vec{Y}_s(\vec{\beta})$ is calculated using the fully implicit, black-oil, coreflood simulator CENDRA[2]. The sensitivity materix, $\mathbf{A}$, is determined by perturbing (in turn) each element in $\vec{\beta}$, and calculating each a_{ij} by a first order finite difference approximation. Finally, $\mathbf{P}$ is calculated through Eq. 3 and thus the relative permeability confidence intervals may be found. Note that no actual experimental data are needed in this analysis.

Our evaluation of the experimental designs comprises the following steps:

1. Select core and fluid properties, and select a set of relative permeability and capillary pressure functions;

2. Select an experimental design (i.e., select a way of conducting the experiments and the types of data and location for those data (in time and space));

3. Perform the covariance analysis, i.e., calculate the confidence intervals around the selected relative permeability functions; and

4. Analyze the confidence intervals with respect to desired accuracy in the estimated functions;

In this manner, quantitative measures of the potential performance of different chosen designs of the experiment can be obtained. We will next discuss items 1 and 2 in the above evaluation procedure.

The adequacy of this approach depends on the suitability of the representation for the relative permeability functions. In two-phase situations, univariate B-splines[14] adequately represent the relative permeability functions[4]. In this work, we have used a bivariate extension of this B-spline representation. The relative permeability surfaces are given by

$$k_{rl}(S_1, S_2) = \sum_{i_1=1}^{m_1+K_1} \sum_{i_2=1}^{m_2+K_2} c_{i_1,i_2} N_{i_1}^{m_1}(S_1, \vec{y}^{\ i_1}) N_{i_2}^{m_2}(S_2, \vec{y}^{\ i_2}), \qquad (4)$$

where $l = w, o, g$, as we will consider water, oil, and gas cases. For convenience we will define $S_1 = 1 - S_l$, and $S_2 = S_w$ if $l \neq w$ and $S_2 = S_g$ otherwise. This representation is a tensor-product expansion of the univariate B-spline in the directions along S_1 and S_2. m_i is the order of the spline along direction i, and K_i is the corresponding number of knots. One can increase the flexibility of the surface by increasing the number of knots (in one or both directions) and/or by increasing the corresponding spline order. The spline coefficients c_{i_1,i_2} will constitute the parameter vector $\vec{\beta}$.

Table 1: Core properties.

Porosity [$frac.$]	0.35
Permeability [mD]	2.0
Core length [cm]	30
Core area [cm^2]	11.22
Oil formation volume factor	1.635
Water formation volume factor	1.0
Water viscosity [cP]	0.34
Oil viscosity [cP]	0.3625
Gas viscosity [cP]	0.0515
Initial Water Saturation [$frac.$]	1.0

The properties of the fluid and core sample considered in this study are given in Table 1. The capillary pressure functions used are shown in Figure 1. In our analysis, we will investigate the determination of the relative permeability functions, assuming that the core and fluid properties as well as capillary pressure functions are known. The analysis works equally well for estimating the accuracy with which other properties may be determined (e.g., the capillary pressure functions); however, such considerations are outside the scope of the present paper. The relative permeability functions used in this study are shown in Figure 2. These functions are tensor-product B-splines of order 3 with 2 knots in each direction, i.e., they are represented by 20 parameters each, giving a total of 60 parameters. Some of the corresponding B-splines do not have support within the saturation area of interest (as $S_w + S_o + S_g = 1$, e.g., $S_w = S_o = 1$ is not a possible saturation combination), which decreases the number of effective parameters to 51. The functions are selected by utilizing three-phase relative permeability points acquired by Oak[9]. The representation in Eq. 4 is fitted to the data through solution of the linear least-squares problem defined by $min\|\vec{k}_{rl}^m - \vec{k}_{rl}^s(\vec{\beta}, S_1, S_2)\|_2^2$, where $\vec{k}_{rl}^m$ is the vector of measured relative permeability values, and $\vec{k}_{rl}^s(\vec{\beta}, S_1, S_2)$ is the corresponding vector of calculated quantities (calculated through Eq. 4). The solution is obtained subject to some constraints, see Eq. 2; we have in this work imposed monotonicity constraints on these relative permeability surfaces.

Table 2: Overview of the experiments considered (W: Water; O: Oil; G: Gas.) All steady-state experiments stops at 80000 min, while the unsteady-state experiments stops at 40000 min.

|	q_w[cc/min]	q_o[cc/min]	q_g[cc/min]	Start time [min]
Experiment 1SS				
WO injection	0.020	0.030	0.000	0.0
WOG injection	0.002	0.010	0.040	10000.0
WOG injection	0.001	0.005	0.150	20000.0
OG injection	0.000	0.002	0.500	30000.0
G injection	0.000	0.000	1.000	50000.0
Experiment 2SS				
WO injection	0.014	0.014	0.000	0.0
WOG injection	0.014	0.014	0.016	10000.0
WOG injection	0.002	0.002	0.040	20000.0
WOG injection	0.001	0.001	0.160	30000.0
G injection	0.000	0.000	0.500	40000.0
G injection	0.000	0.000	1.000	60000.0
Experiment 3SS				
WG injection	0.095	0.000	0.005	0.0
WG injection	0.090	0.000	0.010	10000.0
WG injection	0.050	0.000	0.050	20000.0
WG injection	0.001	0.000	0.099	30000.0
G injection	0.000	0.000	1.000	40000.0
G injection	0.000	0.000	5.000	60000.0
Experiment 1USS				
WO injection	0.020	0.030	0.000	0.0
G injection	0.000	0.000	1.000	10000.0
Experiment 2USS				
WO injection	0.014	0.014	0.000	0.0
G injection	0.000	0.000	1.000	10000.0
Experiment 3USS				
G injection	0.000	0.000	5.000	0.0
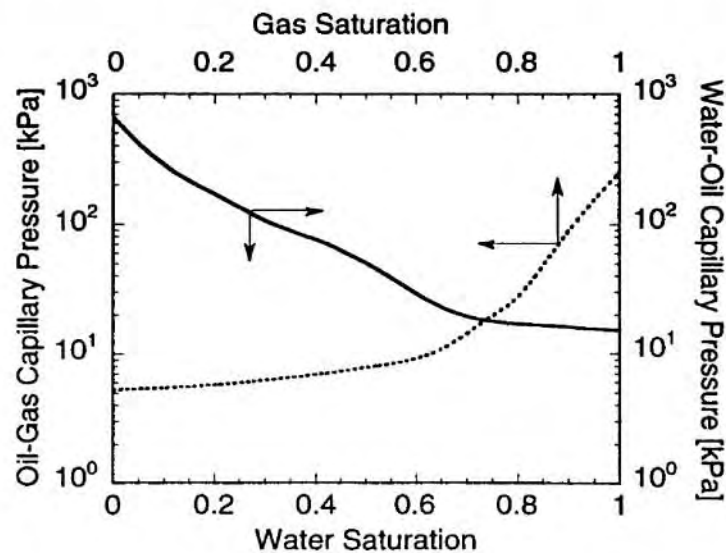
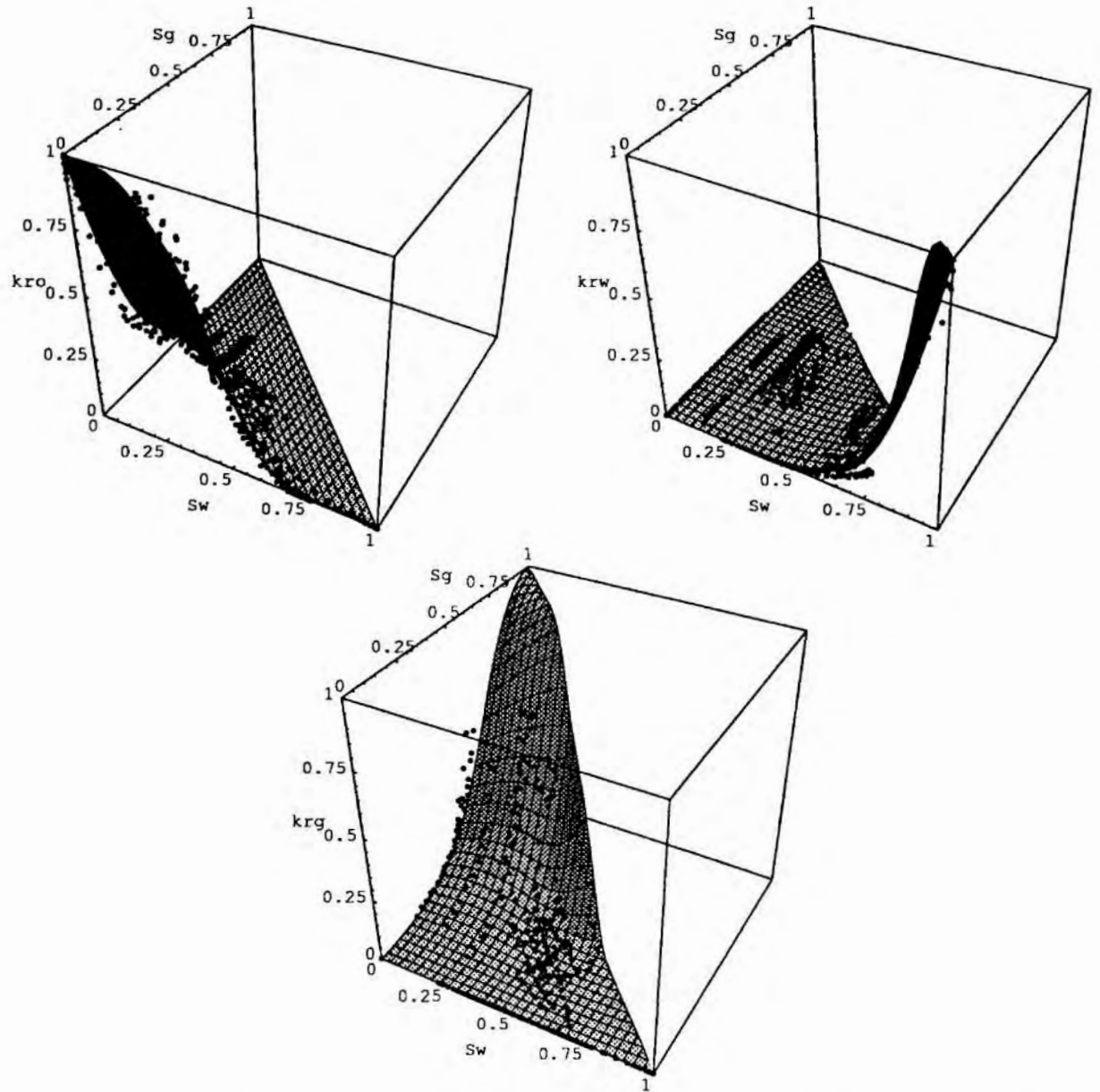Figure 1: Water-oil and oil-gas capillary pressure functions.

Figure 2:   Relative permeabilitity functions used in analysis. Upper left: k_{ro}; upper right: k_{rw}; and lower: k_{rg}

In this work, we have investigated the accuracy with which the relative permeability functions may be determined from 6 different experimental designs, all of which can be considered as modified DDI (decreasing water saturation, decreasing oil saturation, and increasing gas saturation) reservoir condition cases, see Figure 3a). The cases are performed to study how the relative permeabilities in three-phase apparatuses similar to that at RF – Rogaland Research can be determined. In this set-up, three phases can be injected simultaneously at
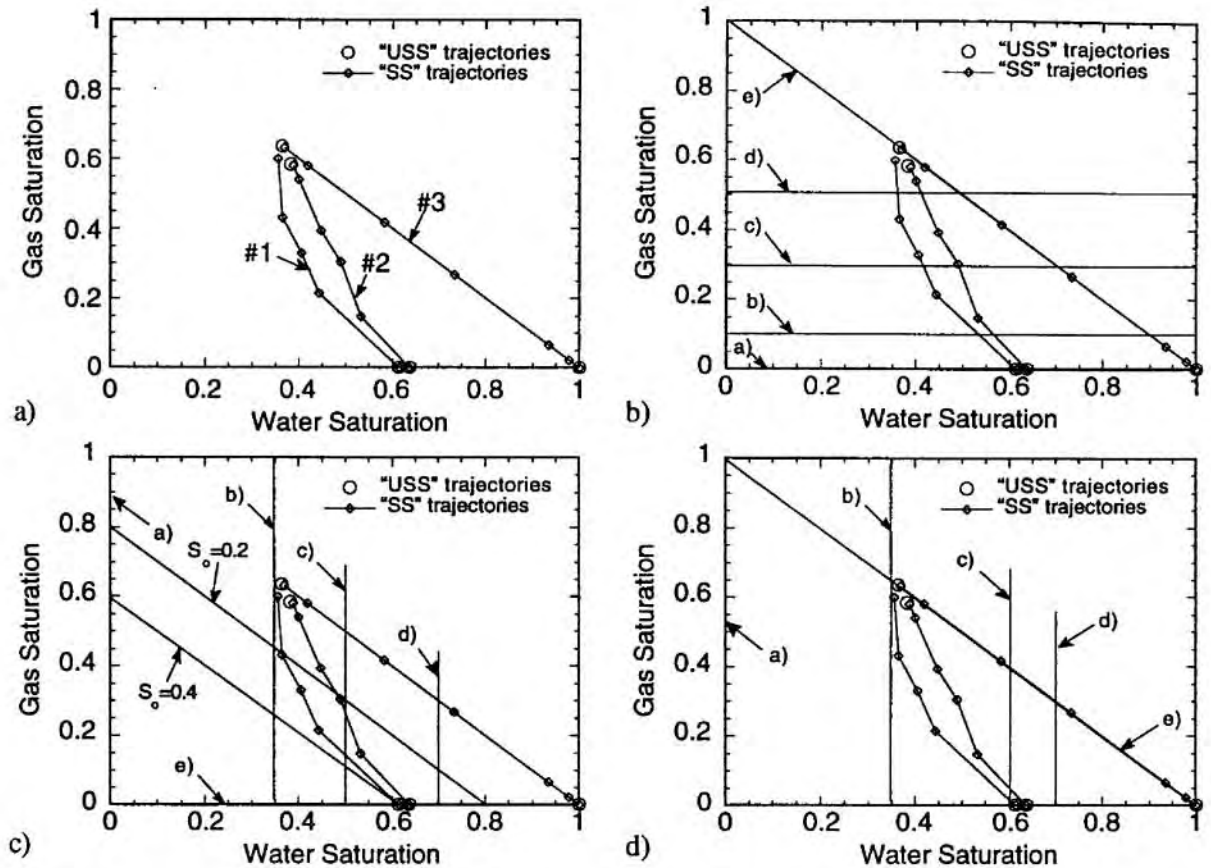
Figure 3: a) Trajectories for all the experiments; b) Sections for study of water relative permeability; c) Sections for study of oil relative permeability; d) Sections for study of gas relative permeability.

reservoir pressure and temperature, and the production of each of the phases and the pressure drop across the core can be measured as a function of time, and the three-phase saturation profiles can be measured at any steady-state situation. Each of the experimental designs is comprised of one to three experiments. Table 2 shows an overview of the injection strategies in all the experiments. The details of these experiments will be discussed next.

In steady-state experiment 1 (1SS; see Table 2 for details on the injection strategy for this experiment), oil and water are first injected into a fully water saturated core sample, and data are "collected" until a near equilibrium situation is reached in both production and pressure drop accross the core (i.e., a close to steady-state situation is attained). Then gas is introduced into the core sample. This is done through a series of steady-state steps. From one steady-state to the next, we decrease the flow rate of liquids (water and oil) and increase the gas rate. In the two last steps, we first maintain the gas flow rate, but let the liquid flow rate go to zero, and then, finally, increase the gas flow rate. The latter is done to establish a high final gas saturation. This procedure follows Oak[9] with only minor modifications. A total of 5 steps are utilized for experiment 1SS. In Figure 3a) the average saturation at the near steady-state condition (i.e, prior to each of the rate changes) is shown as "trajectory" #1. (Note that all of the trajectories starts at unity water saturation.) A similar procedure

is utilized for experiment 2SS (trajectory #2 in Figure 3a)). Experiment 3SS (trajectory #3 in Figure 3a)) is a gas-water injection in a fully water saturated sample. Here, the rate fraction of gas is increased while the water rate is decreased in 6 steps.

Table 3: Overview of the cases considered.

Case	Experiment used	Surfaces considered	# parameters	# datpoints
Case Ia	1SS	k_{rw}, k_{ro}	34	1800
Case Ib	1USS	k_{rw}, k_{ro}	34	1800
Case IIa	1SS, 2SS	k_{rw}, k_{ro}, k_{rg}	51	3600
Case IIb	1USS, 2USS	k_{rw}, k_{ro}, k_{rg}	51	3600
Case IIIa	1SS, 2SS, 3SS	k_{rw}, k_{ro}, k_{rg}	51	5400
Case IIIb	1USS, 2USS, 3USS	k_{rw}, k_{ro}, k_{rg}	51	5400

For the first unsteady-state experiment (1USS), oil and water are first injected into a fully water saturated core sample to establish a two phase oil-water situation in the sample. When a near equilibrium state is obtained, only gas is injected at the same rate fraction as the last gas rate in the corresponding steady-state experiment (i.e., experiment 1SS). A similar procedure is utilized for experiment 2USS. For experiment 3USS gas is injected into a fully water saturated core sample in only 1 step. The end points for gas injections as well as oil-water equilibrium average saturations are shown in Figure 3a) for the three unsteady-state type experiments.

From the 6 experiments we form 6 different experimental designs (referred to as cases) for consideration, see details in Table 3. In the analysis of each of the cases, we assume that we measure production of two phases (water and oil), and the pressure drop across the core as a function of time. The measurement errors are taken to be $\sigma_V = 0.005$ PV and $\sigma_{\Delta P} = 20$ kPa for the produced phase volumes and the pressure drop, respectively. In Case Ia we investigate determination of the water and oil relative permeability surfaces with data from experiment 1SS. I.e., we assume that the gas relative permeability function is known *a priori*, and investigate only the determination of the water and oil relative permeabilities. The dimension of $\vec{\beta}$ is 34. Case Ib is the corresponding unsteady-state case (i.e., using data from experiment 1USS). For Case Ia and Ib we have chosen 1200 production data and 600 pressure data. In Case IIa, we study the determination of all relative permeability surfaces using data from experiments 1SS and 2SS; Case IIb is the corresponding unsteady-state case. Finally, in Case IIIa, we investigate the determination of all of the surfaces from experiments 1SS, 2SS, and 3SS. Again, Case IIIb is the corresponding unsteady-state case; see Table 3 for details.

Results and Discussion

The results from each of these cases are shown in Figure 4 to 6. The figures are constructed to compare the performance of steady-state and unsteady-state type experiments. For each surface the results are shown as cross sections, e.g., the water relative permeability surface with confidence intervals are shown for constant values of the gas saturations in Figures 4a) to 4e). Each of the selected sections are plotted in Figure 3b) together with all the trajectories
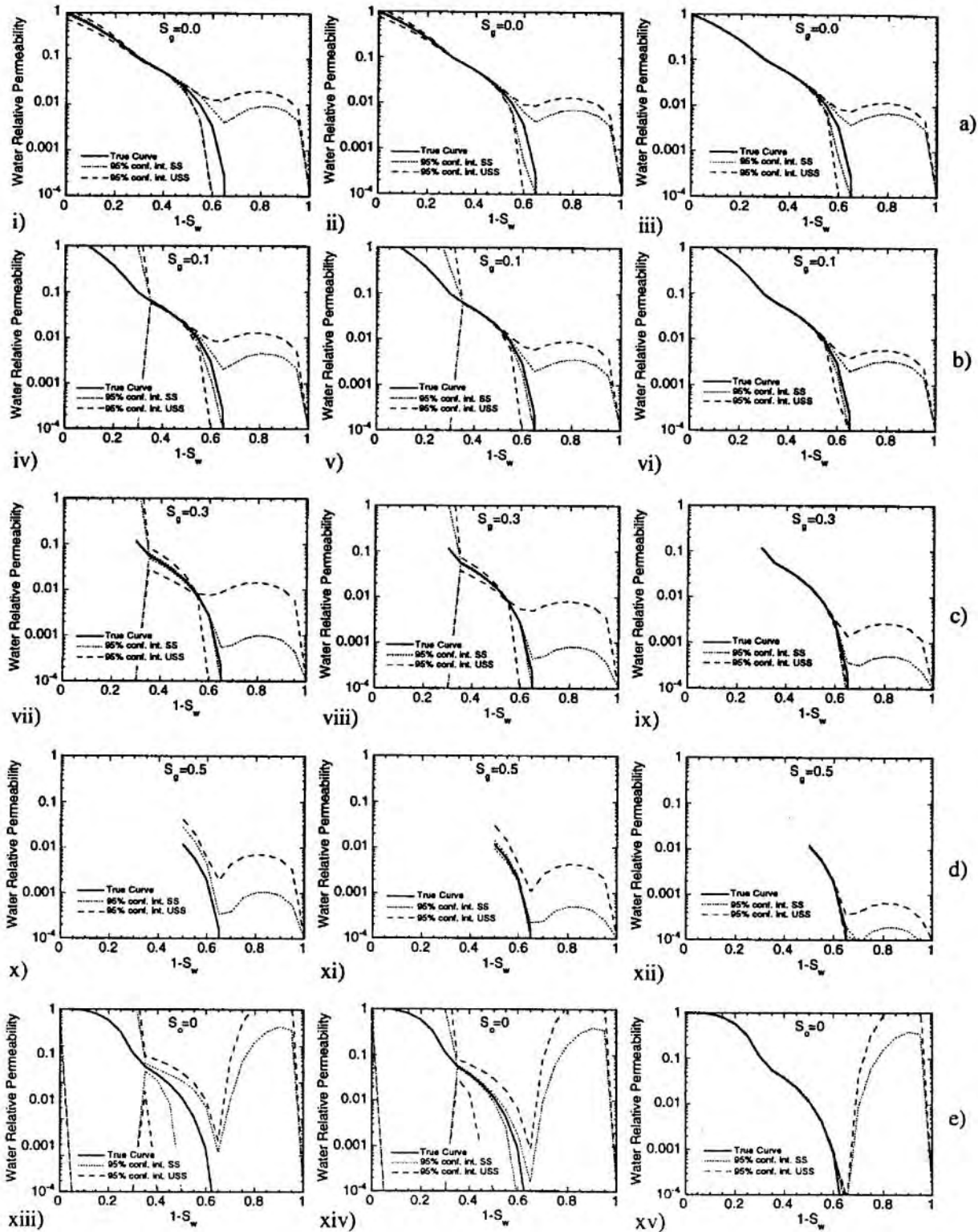
Figure 4: Water relative permeability sections for all the cases. Plots in left column shows results for Case Ia and Ib, in the middle column for Case IIa and IIb, and in the right column for Case IIIa and IIIb. See Figure 3b) for details on the sections.
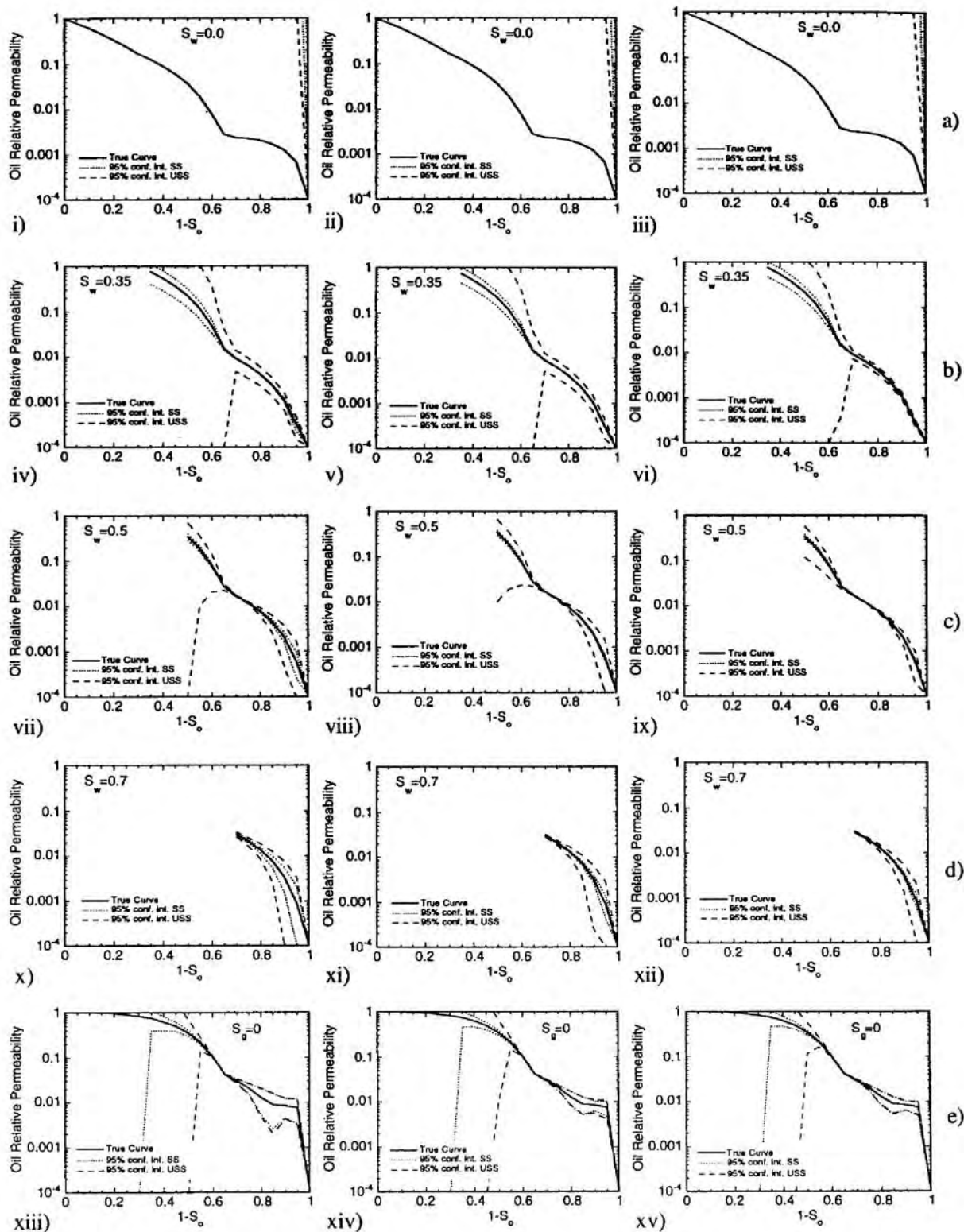
Figure 5: Oil relative permeability sections for all the cases. Plots in left column shows results for Case Ia and Ib, in the middle column for Case IIa and IIb, and in the right column for Case IIIa and IIIb. See Figure 3c) for details on the sections.

(both from steady-state as well as unsteady-state type experiments). The corresponding results for determination of the oil relative permeability are plotted in Figure 5a) to 5e), with cross sections in Figure 3c), and, finally, the results for the gas relative permeability are shown in Figure 6a) to 6e), with cross sections in Figure 3d).

Note that each relative permeability surface appears to be well determined whenever its "own" phase saturation is zero. In our analyses we have utilized the *a priori* information that $k_{ri}(S_i = 0) = 0$. Consequently, the corresponding parameters are eliminated from the covariance analysis, leading to zero confidence intervals whenever $S_i = 0$.

An overall observation is that the relative permeabilities are well determined in saturation regions corresponding to regions represented in the data. For the cases considered here, this region is approximately given by the triangle defined by the intervals $S_w \in [0.3, 1]$ and $S_g \in [0, 0.6]$, and the line $S_o = 0$; see trajectories in Figure 3a) and Figures 4-6.

For $S_g = 0$, the confidence intervals of the water relative permeability are narrow (i.e., k_{rw} is expected to be well determined from the data) for all the cases in a saturation region from unity down to about $S_w = 0.3$. This is the saturation region which is represented in the data from experiments 1SS, 2SS, 1USS, and 2USS; see Figures 4a). For Case Ia, Ib, IIa, and IIb, the water relative permeability will only be well determined in a relatively small S_w-interval whenever $S_g > 0$; see Figure 4b)-d). The reason for this is that the data from the experiments along trajectories #1 and #2 will only reveal relative permeability information in a saturation region close to the trajectories. This means that we should not expect to be able to determine the water relative permeability with any high degree of accuracy for water saturations outside the interval $S_w \in [0.3, 0.6]$, whenever $S_g > 0$. For example, for Case Ia, the confidence interval is relatively large for S_w values higher than 0.6 for $S_g = 0.3$; see Figure 4vii). However, as data along trajectory #3 is added in Case IIIa and IIIb, the water relative permeability surface becomes well determined for S_w values higher than 0.4 for any fixed value of the gas saturation, see Figures 4iii), 4vi), 4ix), and 4xii). Note that while k_{rw} was very poorly determined along the gas-water axis from data from Case Ia, Ib, IIa, and IIb, data from Case IIIa and IIIb determine the relative permeability well along this axis for gas saturation higher than 0.6; compare Figure 4xiii) and 4xiv) with 4xv). Also, note that steady-state type data better determine the water relative permeability surfaces for all the cases and for all the selected sections (frequently by an order of magnitude).

For all the cases, the oil relative permeability is well determined along parts the oil-water axis ($S_g = 0$), see Figures 5e). Generally, k_{ro} is well determined in saturation areas close to the trajectories for the particular case. For example, for $S_w = 0.5$ (see Figures 5c)), the k_{ro} is relatively poorly determined for $S_o \in [0, 0.3]$, as this saturation interval is not represented in the data. For S_o approximately between 0.3 and 0.4, k_{ro} is well determined. This area corresponds to the trajectories #1 (and #2), see Figure 3c) for details on oil saturation vs. trajectory saturations. Again, steady-state type data determine the surface better than unsteady-state data.

For Case IIa and IIb, the gas relative permeability is quite well determined for saturation values corresponding to the trajectories #1 and #2, see Figures 6i), 6iii), 6v), 6vii), and 6ix). However, for high water saturation values, as well as along the water-gas axis, k_{rg} is poorly determined, see Figures 6v) and 6vii). This is because this saturation region is not represented in the data used in Case IIa and IIb. When the gas injection is added (Case IIIa and IIIb), these regions becomes well determined (see Figures 6viii) and 6x)); in fact, the gas relative permeability is quite well determined for approximately $S_w \geq 0.35$ and $S_g < 0.6$.
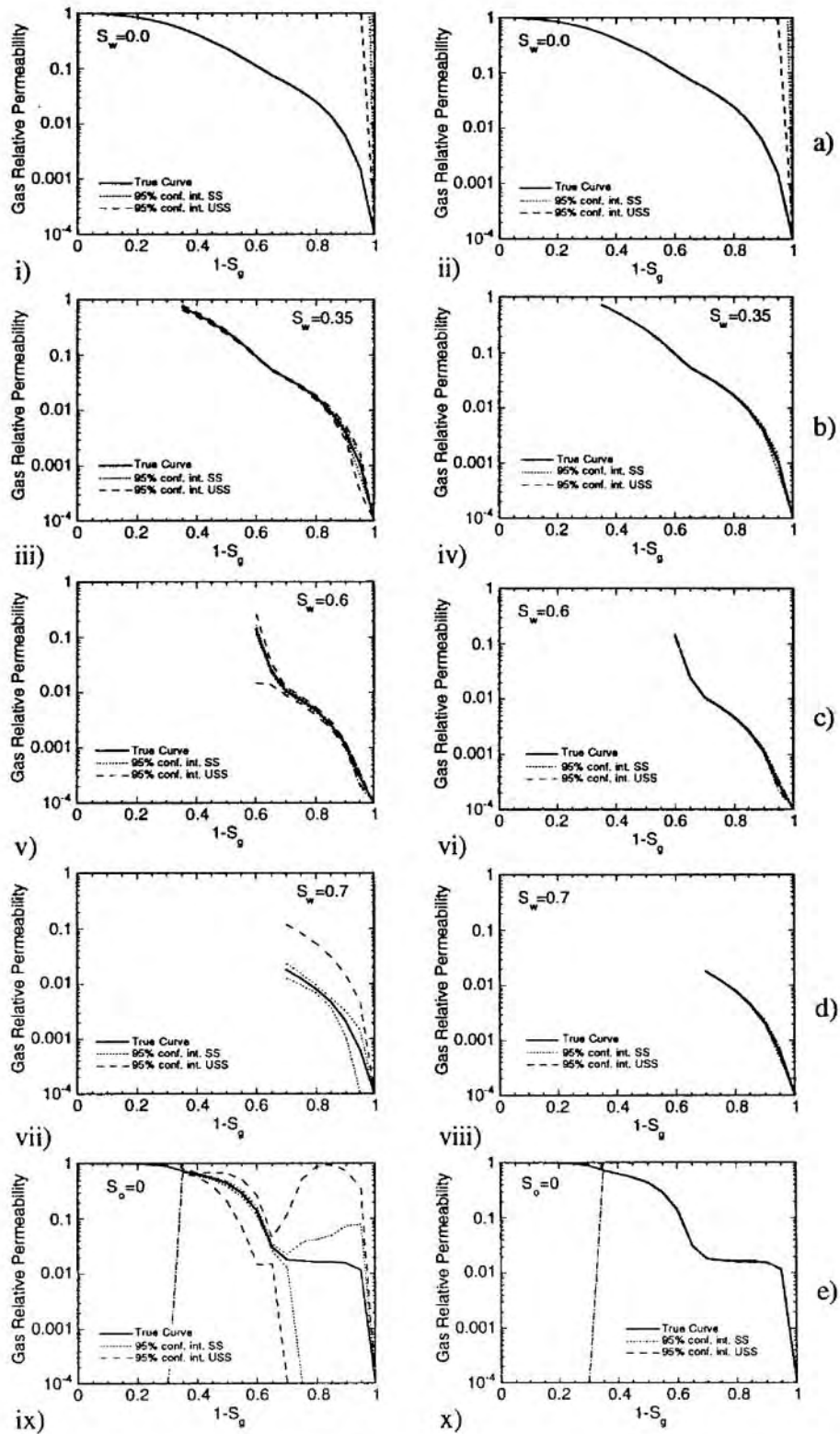
Figure 6: Gas relative permeability sections for all the cases. Plots in left column shows results for Case Ia and Ib, in the middle column for Case IIa and IIb, and in the right column for Case IIIa and IIIb. See Figure 3d) for details on the sections.

Although most pronounced for Case IIa and IIb, the steady-state type data are superior to the unsteady-state type.

Although we limit here the discussion to 6 DDI experimental designs, this approach can be utlized to design experiments of any kind, and the estimation of capillary pressure may also be considered. The outlined method is particularly fruitful for the design of three-phase relative permeability experiments for field applications. In a reservoir engineering context, one may know reasonably well the saturation region that is expected to occur in the reservoir. While it can be quite acceptable to have poorly determined three-phase relative permeabilitites outside this "window," it is imperative to accurately determine the functions within. Our methodology provides a quantitative means for designing experiments leading to accurate relative permeability determination in saturation regions of interest.

Conclusions

1. A systematic method for quantitative evaluation of designs of three-phase relative permeability experiments leading to accurate determination of the relative permeability surfaces has been presented. The evaluation procedure is based on a linearized covariance analysis, and can consider data from several three-phase experiments simultaneously.

2. Six different DDI experimental designs have been analyzed. The analysis show that from the DDI designs considered here, we are able to determine the relative permeability surfaces accurately in a relatively large saturation region, even for a limited number of experiments. Also, the inclusion of water-gas data seems to potentially give significant improvements in analyses leading to relative permeability estimates.

Nomenclature

a_{ij}	Element in sensitivity matrix
$\mathbf{A}$	Sensitivity matrix
$\vec{b}$	Constraint vector
$\vec{\beta}$	Vector of parameters in representation of relative permeabilities
c	Spline coefficients
$\mathbf{C}$	Covariance matrix
$\mathbf{G}$	Constraint matrix
J	Objective function
k	Permeability
K	Number of knots
m	Spline order
N	Normalized B-spline basis function
S	Saturation
$\sigma_{\Delta P}$	Measurement error in the pressure drop data
σ_V	Measurement error in the production data
$\mathbf{P}$	Covariance matrix of parameters
$\vec{y}$	Spline partition

| $\vec{Y}$ | Vector of measured or simulated data |
| **W** | Weighting matrix |

Subscripts / Superscripts

c	Capillary
g	Gas
m	Measured
o	Oil
r	Relative
s	Simulated
w	Water

Acknowledgements

References

[1] Bard, Y.: *Nonlinear Parameter Estimation*, Academic Press, Inc., Washington, DC (1974).

[2] Guo, Y., Nordtvedt, J.E., Olsen, H.: "Development and Improvement of CENDRA+," Report RF-183/93, Confidential.

[3] Johnson, E.F., Bossler, D.P., Naumann, V.O.: "Calculation of Relative Permeability from Displacement Experiments" *Trans.*, AIME, 1958, 370.

[4] Kerig, P.D., Watson, A.T.: "Relative Permeability Estimation From Displacement Experiments: An Error Analysis," *SPE Reservoir Engineering*, Jan. 1986, 175.

[5] Mejia-Velazquez, G.M.: "A Method for Estimating Three-Phase Flow Functions," *PhD Dissertation*, Texas A&M University, College Station, TX, Aug. 1992.

[6] Mejia, G.M., Mohanty, K.K., Watson, A.T.: "Use of *In Situ* Saturation Data in Estimation of Two-Phase Flow Functions in Porous Media," *Journal of Petroleum Science and Engineering*, **12**, 1995, 233.

[7] Nordtvedt, J.E., Mejia, G., Yang, P.-H., Watson, A.T.: "Estimation of Capillary Pressure and Relative Permeability Functions From Centrifuge Experiments," *SPE Reservoir Engineering*, Nov. 1993, 292.

[8] Nordtvedt, J.E., Urkedal, H., Watson, A.T., Ebeltoft, E., Kolltveit, K., Langaas, K., Øxnevad, I.E.I.: "Estimation of Relative Permability and Capillary Pressure Functions

Using Transient and Equilibrium Data From Steady-State Experiments," *Reviewed Proceedings of the 1994 International Symposium of the Society of Core Analysts*, Stavanger, Norway, September 12-14, 1994 197.

[9] Oak, M. J.: "Three-Phase Relative Permeability of Water-Wet Berea," *paper SPE 20183 presented at the SPE/DOE Seventh Symposium on Enhanced Oil Recovery*, Tulsa, OK, April 22-25, 1990.

[10] Oak, M. J., Baker, L. E., Thomas, D. C.: "Three-Phase Relative Permeability of Berea Sandstone," *J. Pet. Tech.*, 1990, 1054.

[11] Richmond, P.C., Watson, A.T.: "Comparison of Implicit and Explicit Methods for Interpreting Displacement Data," *SPE Reservoir Engineering*, Aug. 1990, 389.

[12] Richmond, P.C., Watson, A.T.: "Estimating Multiphase Flow Functions From Displacement Experiments," *SPE Reservoir Engineering*, May 1990, 121.

[13] Sarem, A. M.: "Three-Phase Relative Permeability Measurements by Unsteady-State Method," *Soc. Pet. Eng. J.*, 1966, 199.

[14] Schumaker, L. L.: *Spline Functions: Basic Theory*, John Wiley & Sons, New York (1981).

[15] Watson, A.T., Richmond, P.C., Kerig, P.D., Tao, T.M.: "A Regression-Based Method for Estimating Relative Permeabilities From Displacement Experiments," *SPE Reservoir Engineering*, Aug. 1988, 953.